

SIMPLE BUT EFFECTIVE TREE STRUCTURES FOR DYNAMIC PROGRAMMING-BASED STEREO MATCHING

Michael Bleyer and Margrit Gelautz

*Institute for Software Technology and Interactive Systems, Vienna University of Technology
Favoritenstrasse 9-11/188/2, A-1040 Vienna, Austria*

Keywords: Stereo matching, tree-based dynamic programming, fast stereo method.

Abstract: This work describes a fast method for computing dense stereo correspondences that is capable of generating results close to the state-of-the-art. We propose running a separate disparity computation process in each image pixel. The idea is to root a tree graph on the pixel whose disparity needs to be reconstructed. The tree thereby forms an individual approximation of the standard four-connected grid for this specific pixel. An exact optimum of a predefined energy function on the applied tree structure is determined via dynamic programming (DP), and the root pixel is assigned to the disparity of optimal costs. We present two simple tree structures that allow for the efficient calculation of all trees' optima with only four scanline-based DP passes. These simple trees are designed to capture all pixels of the reference frame and incorporate horizontal and vertical smoothness edges in order to weaken the scanline streaking problem inherent in DP-based approaches. We evaluate our results using the Middlebury test set. Our algorithm currently ranks at the eighth position of approximately 30 algorithms in the Middlebury database. More importantly, it is the currently best-performing method that does not use image segmentation and is significantly faster than most competing algorithms. Our method needs less than a second to determine the disparity map for typical stereo pairs.

1 INTRODUCTION

Stereo vision represents an inexpensive way for reconstructing three-dimensional information from the surrounding environment and is therefore of vital importance for a large number of vision applications. Unfortunately, the key step in stereo vision, i.e. the stereo matching problem, cannot be regarded as solved. Factors that complicate the matching process include image noise, untextured regions and the occlusion problem. Although there is a large body of literature, choosing a stereo algorithm for a practical application is still difficult. While state-of-the-art methods are computationally rather demanding, fast techniques generate significantly worse results. This paper proposes an algorithm that represents a good compromise between these conflicting requirements.

Stereo techniques are commonly divided between local and global methods. Local algorithms are computationally cheap, but they can typically not compete with state-of-the-art results. We therefore focus our discussion on the latter category. A more complete review of stereo methods is, however, given in (Scharstein and Szeliski, 2002).

Global algorithms transform the stereo matching

task into an optimization problem. They seek for a disparity map D that minimizes a predefined energy functional $E(D)$, which is typically in the form of

$$E(D) = E_{data}(D) + E_{smooth}(D). \quad (1)$$

Here, the data term E_{data} assesses the agreement of the disparity solution with the input images by computing a match measurement. In addition, the smoothness term E_{smooth} imposes a penalty on spatially neighbouring pixels carrying different disparity labels. This term is motivated by the fact that neighbouring image points are highly correlated, i.e. they are likely to have similar disparities. A natural choice for a pixel's neighbourhood is the four-connected neighbourhood structure, so that a pixel's disparity is biased towards the disparities of its closest two horizontal and two vertical neighbours. This neighbourhood system leads to the standard four-connected grid shown in Figure 1a.

Optimization of (1) is known to be NP-complete for discontinuity-preserving smoothness functions. Modern stereo techniques commonly apply graph-cuts (Boykov et al., 2001) or belief propagation (Sun et al., 2003) to approximate such energies. Methods that build upon these minimization schemes currently represent the state-of-the-art in stereo match-

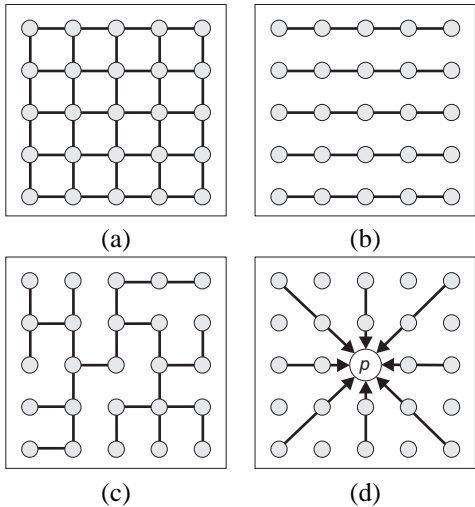


Figure 1: Grid structures of previous approaches. Nodes represent pixels, while edges indicate that the smoothness function operates on the adjacent nodes. (a) Four-connected grid. (b) Scanline-based DP approaches. (c) Tree-based DP proposed by (Veksler, 2005). (d) Approach of (Hirschmüller, 2005) to derive the disparity of pixel p .

ing (Scharstein and Szeliski, 2002). However, a severe limitation of these optimization algorithms is that they are computationally rather expensive. Especially for the graph-cut approach, calculation of a single disparity map can still take several minutes.

To bypass the NP-complete optimization problem, classical DP approaches (Bobick and Intille, 1999; Ohta and Kanade, 1985; Wang et al., 2006) adopt a greatly simplified neighbourhood structure in their smoothness terms. They enforce smoothness only within, but not across horizontal scanlines. The corresponding grid graph is illustrated in Figure 1b. Since there is no interconnection between horizontal scanlines, an energy minimum for this grid structure can be derived by computing the optimum for each scanline separately. The exact optimum of (1) on each individual scanline is then determined using DP. Such approaches are favourable for their excellent computational speed. Skipping the vertical smoothness edges, however, leads to the well-known scanline streaking effect. This inherent problem represents a major reason for the bad reconstruction quality of DP in comparison to the state-of-the-art.

Recently, (Veksler, 2005) proposed approximating the four-connected grid via a tree. The motivation is that efficient DP-based optimization also works on tree structures. Roughly spoken, the tree is constructed by discarding edges that show a high gradient in the intensity image from the four-connected grid. In contrast to scanline-based DP, horizontal and vertical edges are treated symmetrically, which weakens

the streaking problem. Nevertheless, as can be seen from Figure 1c, a large number of edges have to be sacrificed in order to obtain a tree structure. The information of these edges remains unused, which is most likely the reason for the only average results of this method. Subsequent work (Deng and Lin, 2006; Lei et al., 2006) combines tree-based DP with colour segmentation. These algorithms improve the results on standard images such as the Middlebury set (Scharstein and Szeliski, 2002). They, however, fail if segments overlap disparity discontinuities.

A different approach to handle the streaking problem is to compute multiple DP passes. Two-pass methods (Gong and Yang, 2005; Kim et al., 2005) first apply DP on the horizontal scanlines and use the results to bias the second pass, which operates on the vertical scanlines. While horizontal streaks are reduced, these algorithms introduce vertical streaks, and their scanline-based nature is clearly visible in the resulting disparity maps.

(Hirschmüller, 2005) proposed a hybrid approach between local and global methods. The disparity of each pixel is computed using the winner-takes-all strategy, i.e. without considering the disparity assignments of neighbouring pixels. Instead of aggregating matching costs from spatially surrounding pixels, the algorithm computes DP paths from various directions towards each pixel p as shown in Figure 1d. Cost aggregation is then performed by summing up the individual path costs. In Hirschmüller's approach, the disparity of an image point is influenced by only a small subset of the whole image's pixels. This represents a problem if none of the paths captures enough texture to provide a clear cost minimum at the correct disparity. To weaken this problem, Hirschmüller proposed increasing the number of paths. Nevertheless, this results in higher computational demands and only partially represents a remedy to the problem. In a subsequent paper (Hirschmüller, 2006), he addressed this problem using image segmentation.

2 THE SIMPLE TREE METHOD

The algorithm proposed in this paper performs a separate disparity computation for each individual pixel. We apply an individual tree construction in order to determine the disparity of a single pixel. The tree's root node is formed by the pixel whose disparity needs to be computed. Although our trees prove to be effective, their structure is relatively simple. (Hence, we call our algorithm the Simple Tree Method.) For now, it is only important to know that a tree spans all pixels of the reference frame. A global minimum of

an energy function that operates on the tree structure is determined via DP. We then look up the disparity that lies on this energy minimum in the root node. Finally, this disparity is assigned to the image point for which we performed the disparity computation.

In comparison to (Hirschmüller, 2005), our algorithm assigns disparities based on the exact solution of a clearly defined optimization problem. This might represent a more “meaningful” result than selecting the minimum of summed-up path costs. More importantly, we use tree structures that incorporate all pixels of the reference image. A pixel’s disparity is therefore influenced by all other pixels and not just by a subset thereof. This is what (Veksler, 2005) refers to as “truly global”. Practically spoken, our algorithm does not show the problem of missing image features that help to disambiguate a pixel’s disparity, which is specifically important in less textured image regions.

In the context of (Veksler, 2005), the most distinct difference is that we do not apply a single tree to compute the disparities of all pixels at once, but design more flexible trees that vary their grid structures with the spatial position of the pixel under consideration. Obviously, we also share the disadvantage of losing a large number of edges by approximating the four-connected grid via a tree. However, as will be shown in this section, we address this problem by using two complementary tree structures, each of which incorporating a complementary set of edges.

The remainder of this section is organized as follows. We start by defining our energy function (section 2.1). We then present the tree structures applied in our approach (section 2.2). DP on a tree is reviewed in section 2.3. Efficient optimization of the energy function on our tree structures is discussed in section 2.4. Section 2.5 shows how our algorithm combines two different types of trees. Finally, occlusion handling is addressed in section 2.6.

2.1 Energy Function

Let I be the set of all pixels in the reference frame and \mathcal{D} denote the set of allowed disparity labels. We formulate the stereo matching task as finding a disparity solution D that maps each pixel $p \in I$ to a disparity $d_p \in \mathcal{D}$. The goodness of a disparity map D is evaluated by an energy functional, which is subject to minimization. We define the energy function by

$$E(D) = \sum_{p \in I} m(p, d_p) + \sum_{(p, q) \in \mathcal{N}} s(d_p, d_q). \quad (2)$$

Here, the data term $m(p, d_p)$ computes the pixel dissimilarity of p being assigned to d_p . We implement this function using the sampling-insensitive measure-

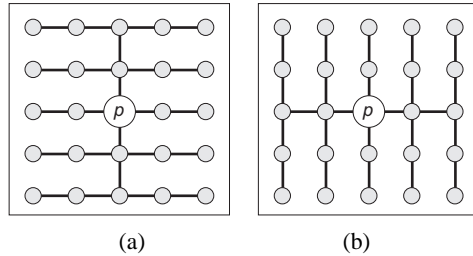


Figure 2: Tree-based approximations of the four-connected grid applied in this approach. Two trees are constructed for each pixel p of the reference frame. (a) Horizontal Tree. (b) Vertical Tree.

ment of (Birchfield and Tomasi, 1998) on RGB values. The smoothness function applied on two pixels p and q that are neighbours according to a predefined set \mathcal{N} is defined by

$$s(d_p, d_q) = \begin{cases} 0 & : d_p = d_q \\ P_1 & : |d_p - d_q| = 1 \\ P_2 & : \text{otherwise.} \end{cases} \quad (3)$$

We impose a user-defined penalty P_1 for small jumps in disparity that do not exceed a value of one pixel. Such jumps commonly occur for slanted surfaces and are typically overpenalized when using the standard Potts model. A second penalty P_2 with $P_2 > P_1$ accounts for penalizing large jumps in disparity that occur at disparity borders. In order to align disparity discontinuities with discontinuities in the intensity image, we compute the value of P_2 by

$$P_2 = \begin{cases} P_3 \cdot P'_2 & : |I_p - I_q| < T \\ P'_2 & : \text{otherwise} \end{cases} \quad (4)$$

with $|I_p - I_q|$ being the summed-up absolute differences of RGB channels. P'_2 , P_3 and T denote predefined constants.

2.2 Simple Tree Structures

Choosing the set of neighbours \mathcal{N} in equation (2) defines the complexity of the resulting optimization problem. In the ideal case, \mathcal{N} is formed by all pairs of spatially neighbouring pixels of the reference image. Since it is known that optimization of the resulting four-connected grid (Figure 1a) is difficult and computationally challenging, we propose finding approximations of this grid in each individual image point. Our approximations are based on trees, i.e. graphs that do not contain cycles. If \mathcal{N} consists of pixel pairs that form a tree on the grid graph, exact minimization of our energy can efficiently be accomplished via DP.

Our first approximation is shown in Figure 2a. The tree is rooted on pixel p whose disparity is computed. It includes all horizontal smoothness edges

of the four-connected grid. In addition, the edges from the vertical scanline on which p is located enforce smoothness in vertical direction. Since horizontal edges dominate in this tree structure, we refer to this tree as the Horizontal Tree.

The second approximation illustrated in Figure 2b can be regarded as the complementary tree structure to the Horizontal Tree. The idea is to include those edges that have been discarded from the four-connected grid in order to derive the Horizontal Tree. The tree is formed by all vertical edges as well as the edges of the horizontal scanline on which p resides. We call this tree the Vertical Tree.

To determine p 's disparity, we optimize our energy function with the set \mathcal{N} being built by all edges of the tree rooted on p . The disparity d_p is then derived by selecting the disparity that lies on the computed optimum. Our algorithm thereby combines the results of Horizontal and Vertical Trees. Section 2.5 shows how this is accomplished.

2.3 DP on a Tree

We can determine an exact optimum of energy (2) on a tree via DP. This works as follows. Let r be the root node of a tree. A minimum value of energy for r at disparity d is computed by passing r and d as arguments to a recursive function $l()$ defined by

$$l(p, d) = m(p, d) + \sum_{q \in v(p)} \min_{i \in \mathcal{D}} (s(d, i) + l(q, i)). \quad (5)$$

Here, the function $v(p)$ returns the siblings of p , i.e. the nodes that have p as their direct predecessor on the path to the root r . Since, by definition, leaf nodes do not have siblings, the function $l()$ can be directly evaluated for these nodes. For a non-leaf node, $l()$ is evaluated when the values of $l()$ have been computed for all its siblings. The algorithm terminates once it reaches the root r . A global energy minimum is computed by $\min_{d \in \mathcal{D}} l(r, d)$, and r 's disparity is determined by $\arg \min_{d \in \mathcal{D}} l(r, d)$.

(Veksler, 2005) has shown that for her energy function the complexity of this algorithm can be reduced to $O(|\mathcal{D}|wh)$ with w and h being the image width and height. However, if we apply the algorithm on a large number of trees, this can easily become computationally intractable.

2.4 DP on Simple Trees

In our approach, we benefit from the simple structure of our trees to significantly improve the computational speed. We show how the optima of all Horizontal Trees are determined with four scanline-based

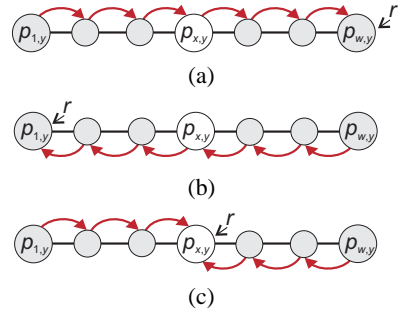


Figure 3: Computation of optimal costs on a scanline. Arrows determine the order in which path costs are computed. In the tree DP algorithm, r denotes the position of the root node. (a) Forward pass. (b) Backward pass. (c) Optimal costs for pixel $p_{x,y}$ are derived by combining costs of forward and backward passes.

DP passes. An analogous construction can be applied for Vertical Trees.

In the first step, we optimize horizontal scanlines separately from each other. The goal is to compute the values of an array C with $C[p, d]$ representing the costs of an optimal disparity solution in which pixel p is assigned to disparity d . In this context, an optimal disparity solution is one that minimizes the energy on individual scanlines. In the following, the values of C are determined with two DP passes as shown in Figure 3. C is needed for further processing.

The first DP pass, which is referred to as forward pass, is similar to that of standard DP methods. We compute the optimal costs for reaching each pixel's disparity from the leftmost pixel of a scanline. These costs are calculated using the following recursion, which represents a simplified form of equation (5):

$$l'(p, d) = m(p, d) + \min_{i \in \mathcal{D}} (s(d, i) + l'(q, i)). \quad (6)$$

Here, q denotes the sibling of p . For the forward pass, this is the pixel to the left of p . In contrast to standard DP methods, $l()$ does not enforce the ordering constraint. This approach is therefore closer related to Scanline Optimization (Scharstein and Szeliski, 2002). The accumulated costs $l'(p, d)$ for each pixel p and disparity d are recorded in an array F .

As a second DP pass, the backward pass determines the costs to reach each pixel's disparity from the rightmost pixel of a scanline. These costs are computed using the function $l'(p, d)$ with p 's sibling q being defined as the pixel to the right of p . An array B stores the accumulated costs of the backward pass.

The optimal costs for each pixel's disparity can be computed from the accumulated costs of forward and backward passes (Kim et al., 2005). Let $p_{x,y}$ denote the pixel at coordinates (x, y) . The energy minimum

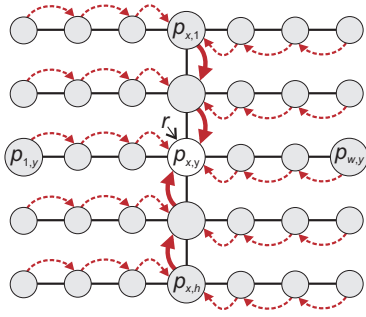


Figure 4: Computation of optimal costs on the Horizontal Tree rooted on pixel $p_{x,y}$. DP only needs to be performed for solid arrows. Optimal values are determined by DP on the vertical scanline using precomputed path costs.

of $p_{x,y}$ at disparity d is derived by expanding the sum in equation (5) at pixel $p_{x,y}$, i.e.

$$\begin{aligned} C(p_{x,y}, d) = & m(p_{x,y}, d) + \min_{i \in \mathcal{D}} (s(d, i) + F[p_{x-1,y}, i]) \\ & + \min_{i \in \mathcal{D}} (s(d, i) + B[p_{x+1,y}, i]). \end{aligned} \quad (7)$$

This is equivalent to

$$C(p_{x,y}, d) = F[p_{x,y}, d] + B[p_{x,y}, d] - m(p_{x,y}, d). \quad (8)$$

It is noteworthy that $\min_{d \in \mathcal{D}} C[p, d]$ is constant for all pixels p of the same scanline. This makes sense, since this value represents the global optimum of our energy function on the scanline. Given that this optimum is unique, we can reconstruct the optimal disparity assignment by computing $d_p = \arg \min_{d \in \mathcal{D}} C[p, d]$.

In the following, we calculate the energy minima for all Horizontal Trees. The basic idea is sketched in Figure 4. We compute the values of an array H with $H[p, d]$ being the energy optimum for the Horizontal Tree rooted on pixel p at disparity d . This value is derived by passing p and d as parameters to a function $l''()$. Considering the special structure of the tree, we define $l''()$ by expanding the sum in equation (5):

$$\begin{aligned} l''(p_{x,y}, d) = & m(p_{x,y}, d) + \min_{i \in \mathcal{D}} (s(d, i) + F[p_{x-1,y}, i]) \\ & + \min_{i \in \mathcal{D}} (s(d, i) + B[p_{x+1,y}, i]) \\ & + \sum_{q \in v'(p_{x,y})} \min_{i \in \mathcal{D}} (s(d, i) + l''(q, i)). \end{aligned} \quad (9)$$

Here, the function $v'(p)$ returns the siblings that are connected to their predecessor via a vertical edge. We use the precomputed values of array C to write

$$\begin{aligned} l''(p_{x,y}, d) = & C[p_{x,y}, d] \\ & + \sum_{q \in v'(p_{x,y})} \min_{i \in \mathcal{D}} (s(d, i) + l''(q, i)). \end{aligned} \quad (10)$$

In the computation of $H[p, d]$ for each pixel p and disparity d , we take advantage of the fact that $l''()$ solely operates on pixels of the same vertical scanline. When interpreting the values of C as the matching costs $m()$ of a DP path, this calculation is, in fact, equivalent to scanline-based DP along the vertical scanlines. Hence, we can use the same strategy as before. That is, we compute forward and backward passes on the precomputed values of C in vertical direction. Finally, the forward and backward passes are combined to determine the energy minima in H .

Computation of the array V representing the optima for the Vertical Tree structure is accomplished equivalently, except that we first optimize vertical scanlines and then operate on the horizontal ones.

Regarding the computational performance, the most expensive part of our algorithm is the calculation of scanline-based DP passes. In a naive implementation, evaluation of $l'(p, d)$ in equation (6) for each pixel p and disparity d takes a complexity of $O(|\mathcal{D}|^2 wh)$. This is an undesirable property when designing a fast algorithm. Analogously to (Hirschmüller, 2005), we reformulate $l'()$ for our energy function as

$$\begin{aligned} l'(p, d) = & m(p, d) + \min(l'(q, d), l'(q, d-1) + P_1, \\ & l'(q, d+1) + P_1, \min_{i \in \mathcal{D}} l'(q, i) + P_2). \end{aligned} \quad (11)$$

Let us compute the values of $l'(p, d)$ at a specific pixel p for each disparity $d \in \mathcal{D}$ using this formulation. The value of $\min_{i \in \mathcal{D}} l'(q, i)$ can be precomputed, so that the complexity of this operation is linear in the number of disparity labels. Consequently, the overall complexity of a DP pass is reduced to $O(|\mathcal{D}|wh)$.

2.5 Combining the Tree Structures

To combine Horizontal and Vertical Trees in our algorithm, we propose the following strategy. We start by operating on the Vertical Tree structure and determine the array V as described in section 2.4. V serves to propagate the results of the Vertical Tree computation to the subsequent calculation of Horizontal Trees. We therefore manipulate the data costs $m()$. The updated matching scores $m'()$ are derived by

$$m'(p, d) = m(p, d) + \lambda \cdot (V(p, d) - \min_{i \in \mathcal{D}} V(p, i)) \quad (12)$$

with λ being a parameter that regulates the influence of the Vertical Trees on the final disparity map. Our update procedure measures the difference between the costs of the solution in which a pixel p is assigned to disparity d and the costs of p 's optimal disparity assignment. If d does not represent an optimal disparity

for p , we impose a penalty on d . The amount of this penalty is proportional to the computed difference. If the difference is large, it is likely that d is the wrong disparity for pixel p . This information is passed to the subsequent calculation by imposing a large penalty. However, if there are pixels whose costs are not much higher than those of the optimal disparity or the optimal disparity is not unique, estimation of p 's disparity is still ambiguous. Such disparities receive only a small penalty, and it is left to the subsequent computation of Horizontal Trees to resolve this ambiguity.

The updated matching scores then represent the input to the calculation of Horizontal Trees. We determine the values of the array H using the modified data costs $m'()$. The final disparity for each pixel p is then selected by $d_p = \arg \min_{d \in \mathcal{D}} H[p, d]$.

2.6 Occlusion Handling

An inherent problem in stereo matching is that of occluded pixels, i.e. pixels visible in one input image, but not in the other one. We cannot expect that our algorithm generates correct depth information in the absence of a matching point. Even worse, the smoothness term of our energy function corrupts disparity estimates for non-occluded pixels by propagating wrong disparity information gathered in occluded regions.

To handle occlusions, we compute two disparity maps. The first disparity map D_R is calculated with the right frame being the reference image. D_R serves solely to identify the occluded pixels of the left image. We use D_R to warp the right image into the geometry of the left view. Pixels of the warped image that do not receive contribution from at least one pixel of the right image are marked as being occluded (Bleyer and Gelautz, 2005). These pixels are recorded in an occlusion map for the left image denoted by O_L . We post-process O_L by deleting occluded pixels whose left and right spatial neighbours are marked as non-occluded. Such pixels typically occur for slanted surfaces that are oversampled in the left image (Ogale and Aloimonos, 2004). These pixels are not occluded, but violate the uniqueness constraint.

The second disparity map D_L is computed with the left image being the reference frame. At this point, we do not attempt to assign occluded pixels of O_L to “correct” disparities. We, however, attempt to avoid that occluded pixels of O_L propagate wrong disparities. We therefore extend the smoothness term of equation (3) by an additional constraint. This constraint is: If at least one of the two neighbouring pixels is marked as occluded in O_L , the smoothness penalty is set to zero. As a consequence, an occluded pixel does not influence the disparity assignments of its neighbour-

ing pixels by imposing the smoothness penalty.

The final disparity map of our algorithm is derived from D_L by overwriting the estimated disparities for occluded pixels with more “meaningful” disparity values. For each occluded pixel p in the occlusion map O_L , we search p 's closest non-occluded pixels on the same horizontal scanline in left and right directions. We determine the minimum of both pixels' disparities and assign this disparity to p .

3 EXPERIMENTAL RESULTS

We use the Middlebury data set (Scharstein and Szeliski, 2002) to evaluate the results of our algorithm. The test set consists of four stereo pairs for which ground truth data is provided. Results of our algorithm on these stereo images are shown in Figure 5. All disparity maps have been generated using constant parameter settings. (The parameters are set to $P_1 = 20$, $P'_1 = 30$, $P_2 = 4$, $T = 30$ and $\lambda = 0.025$.) Obviously, we could improve the results by tuning the parameters for each image pair separately.

The disparity maps in Figure 5 show that our algorithm produces smooth disparity results. Due to the occlusion handling procedure and the algorithm's pixel-based nature, disparity discontinuities appear to be correctly captured. The algorithm also preserves details in the disparity map (e.g., sticks in the cup of the Cones data set). As opposed to other DP approaches, our disparity maps seem to be almost free of streaks. This can be attributed to the structure of our trees that captures horizontal and vertical smoothness edges. Our disparity maps also hardly contain isolated pixels. These are typical artefacts produced by the Semi-Global Approach of (Hirschmüller, 2005) when the DP paths do not capture enough texture. Our approach avoids this problem by applying trees that span all pixels of the reference image. A relatively large error is, however, found to the right of the pink teddy in the Teddy data set. This region is virtually free of texture and image noise biases the results towards the wrong disparity.

We use the Middlebury stereo website (Scharstein and Szeliski, 2002) for a quantitative comparison against competing approaches. Currently, our algorithm ranks on the eighth position of approximately 30 algorithms in the Middlebury online table. Most methods that achieve a better ranking build on graph-cuts or belief propagation. They are far slower than the proposed algorithm, which makes a comparison partially unfair. Moreover, all of the better-performing techniques apply colour segmentation and most of them use the segmentation information as a

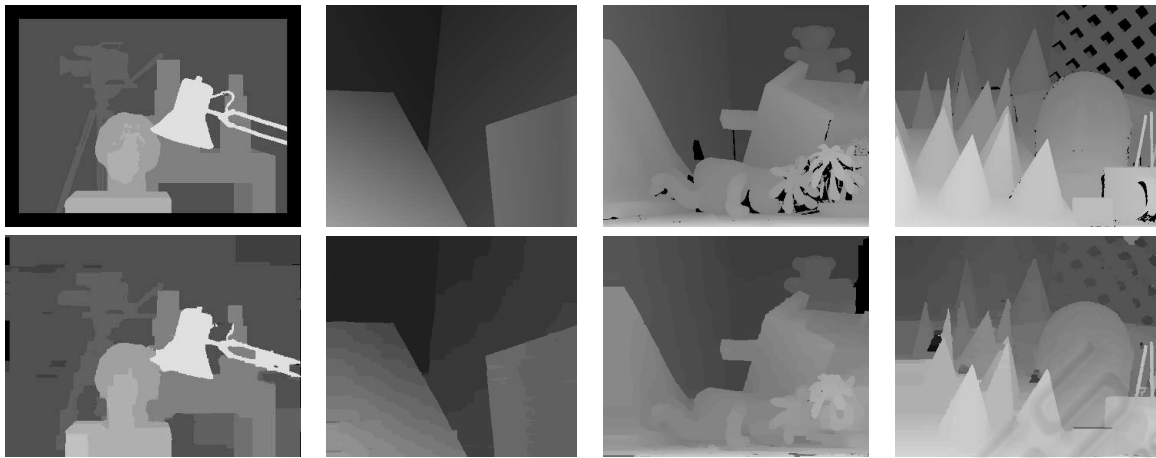


Figure 5: Results of our algorithm on the Tsukuba, Venus, Teddy and Cones image pairs from the Middlebury data set. The upper row shows the ground truth images. The bottom row shows the disparity maps computed by the Simple Tree Method.

hard constraint. While segmentation works well on the Middlebury data set, these algorithms fail in situations such as shown in Figure 6. Applying colour segmentation on the reference image (Figure 6a) leads to segments that overlap disparity discontinuities. Due to these overlapping regions, the segmentation-based algorithm of (Bleyer and Gelautz, 2005), which is one of the top-performers in the Middlebury database, generates erroneous disparity estimates in the proximity of disparity borders (Figure 6c). In contrast to this, the proposed algorithm can correctly capture the disparity discontinuities as the consequence of its pixel-based nature (Figure 6d).

Table 1 gives a quantitative comparison of our algorithm against other DP approaches. These results are obtained from the Middlebury website. Two methods that apply colour segmentation show slightly better results. Apart from the above described problem, it should be noted that performing image segmentation (commonly accomplished using the mean-shift algorithm) is also a computationally costly operation, which can spoil the speed advantage of DP optimization. (Lei et al., 2006) report running times between 10 and 25 seconds on the Middlebury data set with most of the time being consumed by the segmentation overhead. (Hirschmüller, 2006) states that segmentation increases the running time of this approach by 30–50 percent, which makes it likely that also this method is slower than the proposed approach. It can be seen from the table that our technique shows better quantitative results than the Semi-Global Approach of (Hirschmüller, 2005) and significantly outperforms the tree DP method of (Veksler, 2005).

We have run our method on a machine equipped with two dual-core AMD Opteron processors clocked at 2.4 GHz. To take advantage of this multi-core

architecture, we have parallelized the optimization component of our algorithm. We therefore divide the image into even sets of scanlines. The scanline sets are then distributed among the CPUs for performing DP. Overall running times of our implementation range from 0.18 seconds on the Tsukuba stereo pair (384×288 pixels, 16 disparity labels) to 0.57 seconds on the Teddy and Cones sets (450×375 pixels, 60 disparity labels). It is realistic to expect real-time performance as the result of further parallelization, which can, for example, be implemented on the GPU.

4 CONCLUSIONS

The idea of this paper has been to generate a dense disparity map by solving an individual optimization problem for each image point. We approximate the standard four-connected grid in each pixel of the reference frame. Our approximations build on two complementary tree structures, i.e. the Horizontal Tree and the Vertical Tree. We have shown that by exploiting the simple structure of these trees we can efficiently compute the exact solutions of all optimization tasks with only few scanline-based DP passes.

Our algorithm produces disparity maps that are almost free of the streaking problem inherent to DP approaches. Currently, the method is the overall best-performing algorithm in the Middlebury online database that does not apply segmentation. Our algorithm is faster than most competing methods, which typically rely on graph-cuts or belief propagation. We therefore see our algorithm as an alternative method when speed matters. It takes less than a second to compute the disparity map for typical image pairs.

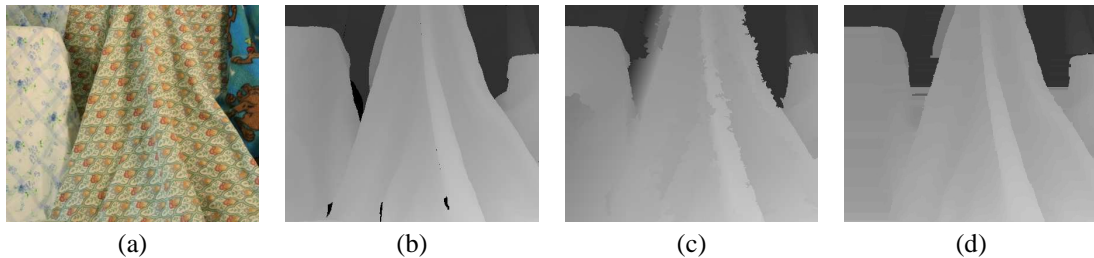


Figure 6: Limitations of segmentation-based methods. (a) Reference view. (b) Ground truth. (c) Result of the segmentation-based algorithm in (Bleyer and Gelautz, 2005). (Percentage of pixels having an absolute disparity error > 1 in non-occluded regions = 4.08.) (d) Result of the proposed method. (Error percentage = 1.80.) More information is given in the text.

Table 1: Rankings of DP approaches in the Middlebury database. Values represent error percentages measured in different image regions. Our algorithm (SimpleTree) is currently the overall best-performing method that does not use segmentation.

Algorithm	Rank	Tsukuba		Venus		Teddy		Cones	
		nooc	all	nooc	all	nooc	all	nooc	all
C-SemiGlob (Hirschmüller, 2006)	5	2.61	3.29	0.25	0.57	5.14	11.8	2.77	8.35
RegionTreeDP (Lei et al., 2006)	6	1.39	1.64	0.22	0.57	7.42	11.9	6.31	11.9
SimpleTree	8	1.86	2.56	0.42	0.76	7.31	12.7	4.00	9.74
SegTreeDP (Deng and Lin, 2006)	10	2.21	2.76	0.46	0.60	9.58	15.2	3.23	7.86
SemiGlob (Hirschmüller, 2005)	12	3.26	3.96	1.00	1.57	6.02	12.2	3.06	9.75
RealTimeGPU (Wang et al., 2006)	19	2.05	4.22	1.92	2.98	7.23	14.4	6.41	13.7
ReliabilityDP (Gong and Yang, 2005)	21	1.36	3.39	2.35	3.48	9.82	16.9	12.9	19.9
TreeDP (Veksler, 2005)	22	1.99	2.84	1.41	2.10	15.9	23.9	10.0	18.3
DP (Scharstein and Szeliski, 2002)	24	4.12	5.04	10.1	11.0	14.0	21.6	10.5	19.1
SO (Scharstein and Szeliski, 2002)	27	5.08	7.22	9.44	10.9	19.9	28.2	13.0	22.8

ACKNOWLEDGEMENTS

This work has been supported by the Austrian Science Fund (FWF) under project P19797.

REFERENCES

- Birchfield, S. and Tomasi, C. (1998). A pixel dissimilarity measure that is insensitive to image sampling. *TPAMI*, 20(4):401–406.
- Bleyer, M. and Gelautz, M. (2005). A layered stereo matching algorithm using image segmentation and global visibility constraints. *ISPRS Journal*, 59(3):128–150.
- Bobick, A. and Intille, S. (1999). Large occlusion stereo. *IJCV*, 33(3):181–200.
- Boykov, Y., Veksler, O., and Zabih, R. (2001). Fast approximate energy minimization via graph cuts. *TPAMI*, 23(11):1222–1239.
- Deng, Y. and Lin, X. (2006). A fast line segment based dense stereo algorithm using tree dynamic programming. In *ECCV*, volume 3, pages 201–212.
- Gong, M. and Yang, Y. (2005). Near real-time reliable stereo matching using programmable graphics hardware. In *CVPR*, pages 924–931.
- Hirschmüller, H. (2005). Accurate and efficient stereo processing by semi-global matching and mutual information. In *CVPR*, volume 2, pages 807–814.
- Hirschmüller, H. (2006). Stereo vision in structured environments by consistent semi-global matching. In *CVPR*, volume 2, pages 2386–2393.
- Kim, J., Lee, K., Choi, B., and Lee, S. (2005). A dense stereo matching using two-pass dynamic programming with generalized ground control points. In *CVPR*, volume 2, pages 1075–1082.
- Lei, C., Selzer, J., and Yang, Y. (2006). Region-tree based stereo using dynamic programming optimization. In *CVPR*, volume 2, pages 2378–2385.
- Ogale, A. S. and Aloimonos, Y. (2004). Stereo correspondence with slanted surfaces: critical implications of horizontal slant. In *CVPR*, pages 568–573.
- Ohta, Y. and Kanade, T. (1985). Stereo by intra- and inter-scanline search. *TPAMI*, 7(2):139–154.
- Scharstein, D. and Szeliski, R. (2002). A taxonomy and evaluation of dense two-frame stereo correspondence algorithms. *IJCV*, 47(1/2/3):7–42. <http://www.middlebury.edu/stereo/>.
- Sun, J., Zheng, N., and Shum, H. (2003). Stereo matching using belief propagation. *TPAMI*, 25(7):787–800.
- Veksler, O. (2005). Stereo correspondence by dynamic programming on a tree. In *CVPR*, pages 384–390.
- Wang, L., Liao, M., Gong, M., Yang, R., and Nister, D. (2006). High quality real-time stereo using adaptive cost aggregation and dynamic programming. In *3DPVT*.